

UDC 544.478.1

DOI: 10.15372/CSD20170614

Effect of Residual Moisture of Alumina on Chemism of Its Chlorination with Carbon Tetrachloride

S. A. YASHNIK¹, N. V. SHIKINA¹, A. V. SAL'NIKOV¹, A. V. ISHCHEIKO¹, Z. R. ISMAGILOV^{1,2}, A. S. NOSKOV¹¹*Boreshkov Institute of Catalysis, Siberian Branch, Russian Academy of Sciences, Novosibirsk, Russia**E-mail: yashnik@catalysis.ru*²*Institute of Coal Chemistry and Material Science, Federal Research Center of Coal and Coal Chemistry, Siberian Branch, Russian Academy of Sciences, Kemerovo, Russia**E-mail: IsmagilovZR@iccms.sbras.ru*

(Received October 01, 2017)

Abstract

The paper carries out a comparative study of the chemical composition of chlorinated alumina produced by chlorination of low-temperature modifications of alumina with carbon tetrachloride and its morphological, structural and acid properties. It is demonstrated that residual moisture has a significant impact on listed properties of chlorinated alumina due to chemism of the reaction between carbon tetrachloride, liberated water vapours, and acid sites of alumina.

Keywords: chlorinated alumina, γ -Al₂O₃, χ -Al₂O₃, carbon tetrachloride

INTRODUCTION

Acid properties of chlorinated alumina surface that determine the activity, selectivity, and stability of its catalytic action in reactions of low-temperature hydroisomerization and alkylation of C₄–C₆ hydrocarbons [1–3] depend on the content of chloride ions and their localization on the Cl–Al₂O₃ surface [4, 5]. The content of chloride ions in Cl–Al₂O₃ catalysts is determined by synthesis conditions, in particular, the nature of the chlorinated compound and chlorination temperature. However, analysis of the results of papers [3, 5–9] demonstrates that chlorine contents in Cl–Al₂O₃ samples produced at the identical temperature of interaction of γ -Al₂O₃ with CCl₄ and HCl are comparable and are 2–3 centres per

nm² [9–11], while acid properties of chlorinated alumina surface are different. The interaction of γ -Al₂O₃ with inorganic Cl-containing compounds ensures generation of Bronsted acid sites (BAS) [7, 10, 12], while reactions with organic matter promote the generation of Lewis acid sites (LAS) [2, 4, 7, 8, 13, 14]. On the other hand, some authors believe that the causes of the formation of BAS in chlorinated alumina are low temperatures of dewatering of alumina [15] and/or its thermal treatment after chlorination [16, 17]. For instance, it is proven that only LAS are generated resulting from chlorination of Al₂O₃ with gaseous chlorine at 700–950 °C [15–17], while hydroxyl groups and base sites are completely absent [16, 17]. The BAS appear in case of cooling of Cl–Al₂O₃ to room temperature without preliminary high-

temperature degassing [16], and also in case of chlorination of Al_2O_3 dried at temperatures not higher than 50°C [15].

The mechanism of interaction of Cl-containing precursor with alumina apparently also depends on the crystalline structure of Al_2O_3 , as it determines the peculiarities of properties of Al_2O_3 , in particular, the density of OH groups and their distribution in the structure [18, 19]. Physicochemical and catalytic properties of Cl- Al_2O_3 on the basis of γ - [5, 7, 8, 10, 12, 13] and η -modifications [20–22] are thoroughly studied; at the same time, χ - Al_2O_3 is not paid much attention to.

This paper discusses the main peculiarities of chlorination of χ - Al_2O_3 with CCl_4 that differ by residual moisture content, and also the effect of residual moisture of χ - Al_2O_3 on textural,

morphological, and acid properties of Cl- Al_2O_3 .

EXPERIMENTAL

Preparation of catalysts

Residual moisture content in χ - Al_2O_3 was varied by thermal treatment of gibbsite (Pikalevsky aluminous factory CJSC, Pikalevo city) at temperatures of 120, 200, 300, 400, 500 and 600°C for 4 h. Table 1 gives residual moisture content, phase composition, specific surface area, and pore volume smaller than 300 nm.

Chlorination of alumina was carried out under flowing conditions. For this purpose, a sample of alumina with a mass of 1 g was loaded into a quartz reactor and subjected to

TABLE 1

Chemical and phase composition, textural and acid characteristics of alumina prepared by gibbsite thermal treatment at different temperatures

Sample number	Calcination temperature, $^\circ\text{C}$	Moisture content, g $\text{H}_2\text{O}/\text{g}$ Al_2O_3	Phase composition, D_{ser}	Textural characteristics ^a			Content of acid centres (LAS/BAS) ^b , $\mu\text{mol}/\text{g}$
				A_{BET} , m^2/g	V_{pore} , cm^3/g	D_{pore} , nm	
1	120	0.307	Gibbsite, >100 nm	0.17	0.002	41.5	–
2	200	0.306	Gibbsite, >100 nm Boehmite, traces	0.22	0.002	40.5	–
3	300	0.114	χ - Al_2O_3 , <5 nm Boehmite, 70 nm	290	0.18	11.5	590 (540/–)
4	400	0.092	χ - Al_2O_3 , 5 nm Boehmite, 70 nm	282	0.22	10.3	790 (540/–)
5	500	0.020	χ - Al_2O_3 , 5.1 nm Boehmite, traces	234	0.20	7.6	710 (520/45)
6	600	0.027	χ - Al_2O_3 , 5.8 nm 10% γ - Al_2O_3	166	0.26	5.6	660 (460/50)
7	700	0.022	χ - Al_2O_3 , 6.5 nm 7.5% γ - Al_2O_3	156	0.24	6.0	630
8	800	0.010	χ - Al_2O_3 , 7.1 nm δ - Al_2O_3	105	0.26	9.8	500
9	900	0.008	κ - Al_2O_3 , 7.7 nm δ - Al_2O_3	108	0.26	9.5	–
10	1000	<0.005	κ - Al_2O_3 (major), 38 nm δ - Al_2O_3 , 7.7 nm	43	0.24	21.7	85

^a A_{BET} is specific surface area, V_{pore} is pore volume, D_{pore} is predominating size of pores; these characteristics are calculated for isotherms of low-temperature nitrogen adsorption.

^bFrom the data of NH_3 thermal desorption in the temperature of 200–600 $^\circ\text{C}$; in brackets there are concentrations of LAS and BAS calculated from areas of peaks of ammonia desorption in the temperature ranges of (200–400)/(530–600 $^\circ\text{C}$), respectively.

dewatering (1 h) under a stream of nitrogen (1.8 L/h) at a temperature of its thermal treatment. Afterwards, a stream of nitrogen, in which chemically pure carbon tetrachloride was fed by LS-301 peristaltic pump was passed through a layer of Al₂O₃ with a rate of 6.5 g/h for 1 h. The total speed of the gas flow was 2.75 L/h, the concentration of CCl₄ in it was 0.015 mol/L. Temperature and time of chlorination were 350 °C and 1 h, respectively. After termination of CCl₄ feeding into a stream of nitrogen, the catalyst was aged in this stream at 350 °C for another 1 h and the sample was cooled in the nitrogen flow to room temperature. Hereinafter, the samples are designated as $\alpha\text{Cl}/\chi\text{-Al}_2\text{O}_3\text{-}T$, where α is chlorine content (mass %), $\chi\text{-Al}_2\text{O}_3$ is a crystalline modification of Al₂O₃, and T is the temperature of dehydration of Al₂O₃ (°C).

Table 2 gives the phase and chemical composition of chlorinated alumina samples, and also their textural characteristics.

Physicochemical methods

The chemical composition of Cl/Al₂O₃- T was studied by X-ray fluorescence analysis method

using ARL analyzer with Rh-anode of X-ray tube. The pH value of the solution, through which the waste gas mixture (at the exit of the reactor) was passed, was analyzed by the potentiometric method using a HI1131 glass pH-electrode and a pH-211 laboratory pH-meter (Hanna Instrument, Germany).

Moisture content in gibbsite samples calcined at various temperatures (120–600 °C) was determined as mass loss after calcining for 2 h at a temperature of 600 °C (Δm) referred to sample mass before calcination (m_0).

Textural characteristics of samples, such as specific surface (A_{BET}) and pore volume (V_{Σ}), were studied by the method of low-temperature adsorption of nitrogen. The measurements of N₂ adsorption/desorption isotherms were carried out using ASAP 2400 automatic volumetric device (Micromeritics, USA).

To determine phase composition of samples X-ray diffraction was used. The powder XRD patterns were recorded on HZG-4C diffractometer (Freiberger Präzisionmechanik, Germany) in the angle range 2θ from 10 to 70° using monochromatic CuK α radiation ($\lambda = 1.54418 \text{ \AA}$). Identification of phases was carried out using

TABLE 2

Chemical and phase composition, textural and acid characteristics of chlorinated alumina prepared from gibbsite samples with different residual moisture content

Sample number	Calcination temperature, °C	Chemical composition, mass %			Phase composition	Textural ^a characteristic			Content of acid centres (LAS) ^b , $\mu\text{mol/g}$
		Al	Cl	Cl/Al		A_{BET} , m ² /g	V_{pore} , cm ³ /g	D_{pore} , nm	
1	200	48.73	4.88	0.076	$\chi\text{-Al}_2\text{O}_3$, 5 nm Boehmite, 70 nm	275	0.19	5.5	10 (7)
2	300	49.11	5.19	0.080	$\chi\text{-Al}_2\text{O}_3$, 5 nm Boehmite, 70 nm	248	0.21	4.8	30 (8)
3	400	49.43	4.38	0.067	$\chi\text{-Al}_2\text{O}_3$, 5 nm Boehmite, 70 nm	230	0.21	4.8	–
4	500	48.33	2.73	0.043	$\chi\text{-Al}_2\text{O}_3$, 5.1 nm Boehmite, traces	176	0.21	4.2	347 (310)
5	600	49.87	3.54	0.054	$\chi\text{-Al}_2\text{O}_3$, 5.8 nm 10 % $\gamma\text{-Al}_2\text{O}_3$	165	0.30	5.7	820 (720)
6 ^c	500	–	0.21	–	$\chi\text{-Al}_2\text{O}_3$, 5.2 nm	165	0.25	5.5	350 (210)

^a A_{BET} is specific surface area, V_{pore} is pore volume, D_{pore} is predominating size of pores; these characteristics are calculated for isotherms of low-temperature nitrogen adsorption.

^bFrom the data of NH₃ thermal desorption in the temperature of 200–600 °C, in brackets there are concentrations of LAS calculated from areas of peaks of ammonia desorption in the temperature range 200–400 °C.

^cSample is prepared by the method of impregnation by carbon tetrachloride with subsequent calcination at static conditions at 350 °C in nitrogen atmosphere.

X-ray Powder Diffraction File JCPDS-ICDD crystallographic database (Win. Ver 1.30, JCPDS ICDD, Swarthmore, PA, the USA, 1997).

The morphology of the samples was studied by high resolution transmission electron microscopy (HRTEM), obtaining micrographs of samples using JEM-2010 electron microscope (JEOL, Japan) with a resolution of 0.14 nm at an accelerating voltage of 200 kV. Samples for the study by HRTEM method were dispersed using ultrasonic treatment and applied onto perforated carbon substrates supported on copper meshes.

The stability of Cl/Al₂O₃-T samples was studied by thermogravimetry/differential thermal analysis (TG/DTA using NETZSCH STA 449 instrument (Netzsch-Geratebau GmbH, Germany). A weighted sample with a mass of 30 mg (powder) was placed into a crucible, a flow of air (50 cm³/min) or helium (100 cm³/min) was fed and heating from 20 to 600 °C with a rate of 10 K/min was carried out.

Surface acidity was studied by the method of ammonia temperature-programmed desorption (NH₃-TPD). The NH₃-TPD experiments were carried out in the flow system equipped with the thermal conductivity detector. A sample with a mass of 100 mg with a fractional composition of 0.25–0.50 mm was mixed with 100 mg of quartz with a similar size of granules. It was then aged under argon flow (30 cm³/min) at a temperature of 350 °C (the temperature of chlorination) within 2 h to remove the adsorbed water. Then it was cooled to a temperature of 75 °C and ammonia was adsorbed blowing out the sample with a mixture of ammonia (0.35 vol. %) in argon for 0.5 h. Afterwards, the sample was blown out with argon (30 cm³/min) to remove ammonia from pores of the catalyst and physically adsorbed ammonia from its surface, and then cooled to room temperature in an argon flow. The NH₃-TPD curve was registered, passing argon through the sample with a rate of 30 cm³/min and heating it from 25 to 700 °C with a rate of 10 °C/min. Calibration by the amount of liberated ammonia was performed by registering the known dose of ammonia under similar conditions. The total surface acidity of samples was assessed according to the number of desorbed ammonia species assuming one-centre ammonia desorption.

RESULTS AND DISCUSSION

Structure and properties of Al₂O₃ dewatered at different temperatures

An increase in the temperature of thermal treatment of gibbsite and χ -Al₂O₃ leads not only to a reduction in residual moisture but also, as it is known, to a change in phase composition of alumina, its textural characteristics and acid properties of the surface.

Gibbsite is aluminium hydroxide with a chemical formula of γ -Al(OH)₃. It crystallizes as large species with a size to 1 μ m longitudinally and a ratio of the form factor of 3–10 (Fig. 1, a) consisting of hexagonal-tabular crystals (see Fig. 1, b) with complex twinned intergrowths at the faces (100) and (110) [23, 24]. Gibbsite has a layered structure, in which a dioctahedral layer of Al³⁺ cations with 2/3 occupied octahedral positions is located between two hydroxyl layers [25–27]. Each Al³⁺ cation has six OH groups in the first coordination sphere; they form a distorted octahedron around Al³⁺ [23, 25]. The X-ray pattern of initial gibbsite sample contains a set of reflexes, which, according to X-ray base, corresponds to gibbsite, or γ -Al(OH)₃, and has a size of coherent scattering regions (D_{CSR}) of not less than 100 nm (see Table 1).

The layered structure of gibbsite begins to decompose at a temperature of 180–220 °C [23–26]. In the X-ray diffraction pattern of a sample exposed to thermal treatment at 200 °C, the intensity of reflexes of gibbsite is somewhat decreased and additional broad reflexes appear. The totality of new reflexes refers to boehmite with D_{CSR} of no more than 100 nm. There are endo-effects with a mass loss at temperatures of 230–250 and 315–330 °C in DTA and TG curves of crystallized gibbsite (Fig. 2). The first endo-effect is driven by gibbsite dehydration related to the removal of crystal water {Al(OH)₃·*n*H₂O → Al(OH)₃ + *n*H₂O} and generation of boehmite {Al(OH)₃ → AlOOH + H₂O}. At 325 °C, anhydrous aluminium hydroxide transforms into χ -Al₂O₃ and structural water is removed {2Al(OH)₃ → χ -Al₂O₃ + 3H₂O}. The X-ray phase composition of samples calcined at 300 and 400 °C (see Table 1) is determined by χ -Al₂O₃ and boehmite with a size of D_{CSR} of not more than 5 and 70 nm, respectively.

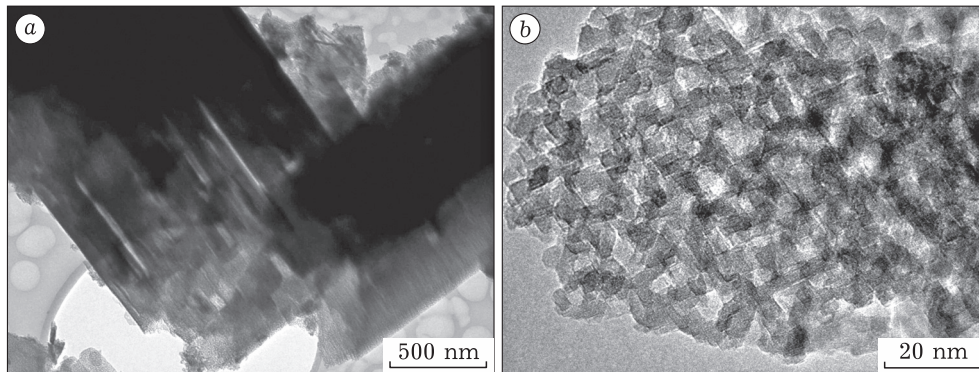


Fig. 1. TEM images of initial gibbsite sample. An increase of 10k (a), 250k (b).

An increase in thermal treatment temperature from 200 °C to 300 and then to 400 °C leads to a three-fold reduction of moisture content in samples, from 0.306 to 0.114 and 0.092 g H₂O/g Al₂O₃, respectively.

Minor mass loss (to 4 mass %) with endo-effect present at 530–540 °C in TG and DTA curves of initial gibbsite sample (see Fig. 2) is related to the transformation of boehmite to γ -Al₂O₃ that proceeds due to the removal of non-stoichiometric oxygen and surface OH groups. XPD method results of a sample calcined at 600 °C, according to which it contains

χ -Al₂O₃ and to 10 % γ -Al₂O₃ with D_{CSR} of no more than 6 nm, confirm this assumption. According to TEM data, the transformation of gibbsite to χ -Al₂O₃ leads to particle dispersion. After calcination at 600 °C, the resulting χ -Al₂O₃ species have the form of hexagonal prisms with a size of 100–150 nm in cross-section (Fig. 3, a). In small numbers, there are even species with a size of about 20–50 nm. The faceting of χ -Al₂O₃ crystals in the main crystallographic directions is not clearly expressed. Species with a clear porous structure and denser particles are present in an approximately equal ratio (see Fig. 3,

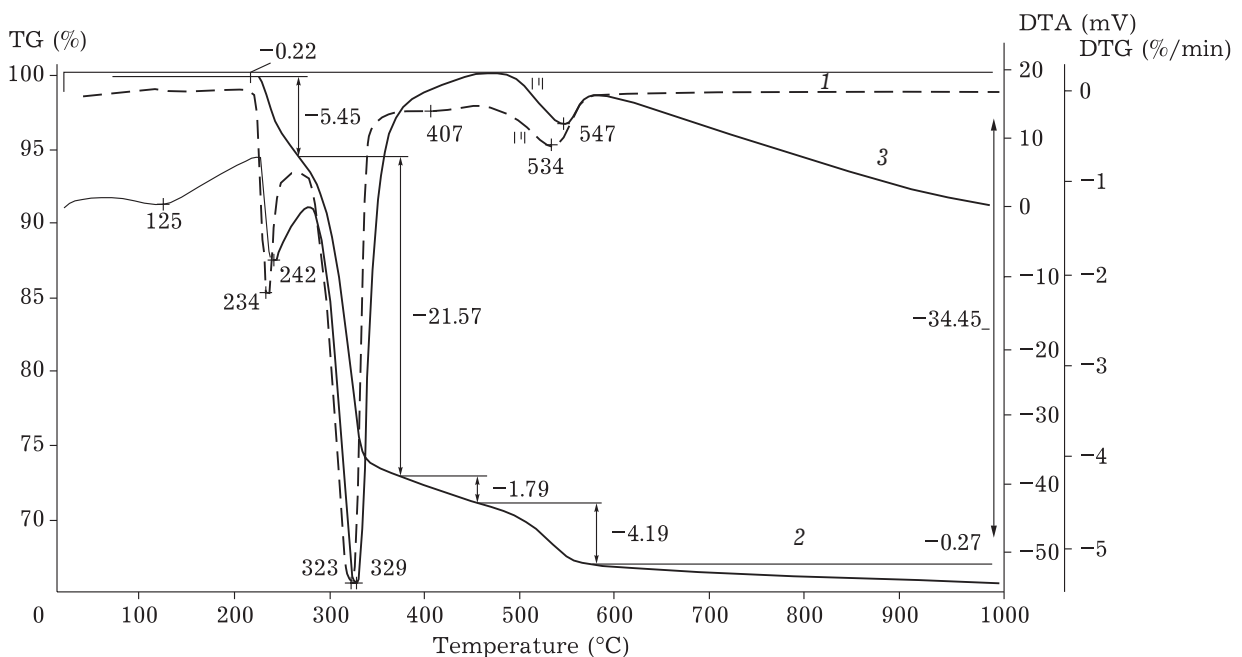


Fig. 2. TG (1), DTG (2) and DTA (3) curves obtained by thermogravimetry of gibbsite.

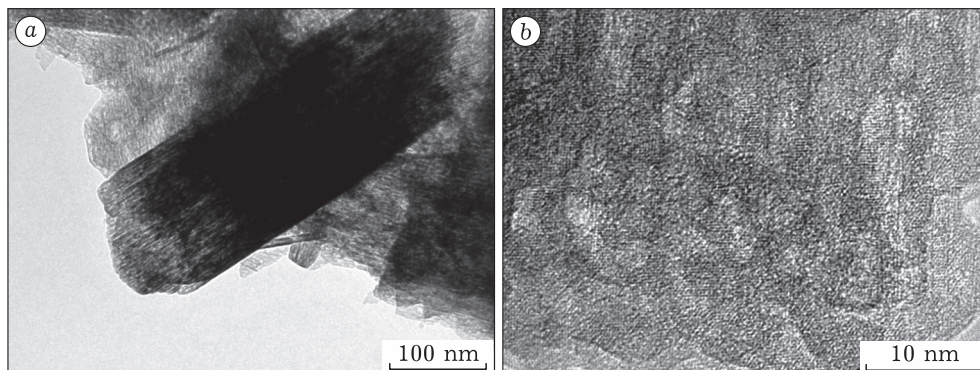


Fig. 3. TEM images of χ - Al_2O_3 sample obtained from Pikalevo gibbsite by thermal treatment at 600 °C. An increase of 10k (a), 250k (b).

b). Cavities, through pores, and facet structure of the particles are clearly visible in the images at a magnification of 250,000 times. Moisture content in samples calcined at 500 and 600 °C is 3–5 times lower compared to those with thermal treatment temperatures of 300 °C.

At higher temperatures, low-temperature χ - Al_2O_3 that usually has a crystalline lattice with a large number of defects [28] undergoes phase transformations converting to κ - Al_2O_3 at 500–800 °C [24–26] and to α - Al_2O_3 at 1000–1200 °C [24–26] without mass loss (crystallization accompanied by exothermic effect). However, in the case of Pikalevo gibbsite sample, a phase transition of χ - Al_2O_3 to κ - Al_2O_3 begins near 800 °C and ends at 1000 °C.

Increasing gibbsite calcination temperature leads to a change in its textural characteristics (Fig. 4). Nitrogen low-temperature adsorption isotherms for gibbsite samples with different thermal treatment temperatures given in Fig. 4, a refer to the IV type that characterizes polymer adsorption of nitrogen in mesoporous materials with pores of 2–50 nm and saturation when approaching the pressure to saturated vapour pressure. It should be noted that the hysteresis loop in nitrogen low-temperatures adsorptions shifts to the region of high pressures with increasing gibbsite thermal treatment temperature (see Fig. 4, a). This shift usually indicates a change in the size and shape of pores in porous materials.

Textural characteristics of alumina change dramatically in generating new crystalline phases in samples, as demonstrated by analysis of data from Table 1. Several temperature re-

gions of thermal treatment of Al_2O_3 , in which phase composition of samples is constant and textural characteristics change poorly, can be identified: 120–200, 300–500, 600–700, 800–900, and 1000 °C. Initial gibbsite samples gave a low specific surface area (no more than 0.2 m^2/g), which is driven by large size of its species and almost an entire lack of pores. The samples are characterized by the developed specific surface area (155–235 m^2/g) in the range of formation and existence of χ - Al_2O_3 (300–700 °C) due to the generation of highly dispersed χ - Al_2O_3 species (5–6.5 nm) penetrated by micro/mesopores (see Fig. 3, b). It should be noted that specific surface area values for gibbsite calcined at 400 and 500 °C calculated according to BET and BJH methods differ between each other approximately by 70–80 %. This implies that the differential distribution curve for pores examines only 20–30 % of mesopores; the rest have a size of less than 3.4 nm and are not displayed in distribution curves (see Fig. 4, b), therefore, the specified samples are finely porous. Pore size distribution in samples calcined to 700 °C has the distinct homogeneous porous nature with maximum pore distribution in the range of 3.8–3.9 nm. Herewith, pore number with these sizes is much higher in samples with calcination temperature (T_{calc}) of 600 and 700 °C than in those calcined at 400 and 500 °C (see Fig. 4, b). However, there is a shoulder in the area of wider pores (4–6 nm) in differential pore size distribution curves for samples calcined at 600 and 700 °C. This causes a significant (in 1.5 times) reduction in specific surface area values of the specified samples compared to samples

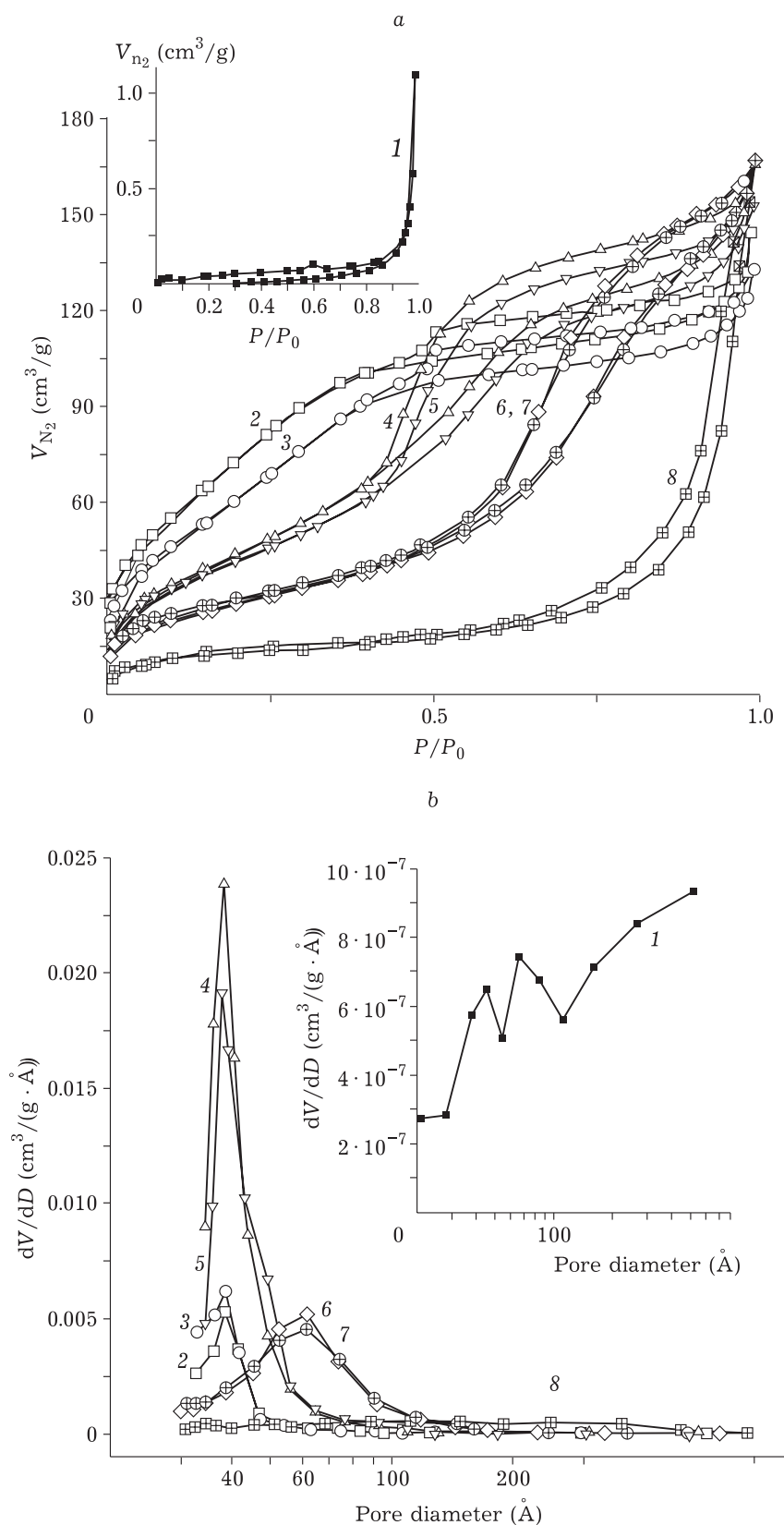


Fig. 4. Adsorption isotherms and differential pore size distribution of initial (1) and calcined gibbsite samples at temperatures of 400 (2), 500 (3), 600 (4), 700 (5), 800 (6), 900 (7), and 1000°C (8).

with treatment temperatures of 400 and 500 °C.

After thermal treatment of a sample at 800 and 900 °C causing transformation of χ -Al₂O₃ to κ -Al₂O₃ and an increase in the size of crystallites (see Table 1), it becomes broad porous with prevailing of pores in the size of 3.5–11 nm (see Fig. 4, b). The volume of thin mesopores in samples with calcination temperatures of 800 and 900 °C is significantly lower compared to those exposed to thermal treatment at 400–700 °C. The average pore size increases 1.5 times, which leads to a decrease in the specific surface area of samples.

The result of calcination of gibbsite at 1000 °C is a considerable enlargement of κ -Al₂O₃ crystallites (to 38 nm) and sintering of small pores, with the result that the sample has a broad porous texture with pores in the range from 10 to 100 nm.

Since the phase composition of gibbsite samples calcined above 700 °C is different from χ -Al₂O₃, then to reveal the effect of residual moisture on chemism of chlorination of χ -Al₂O₃ with carbon tetrachloride samples with calcination temperatures of 300–600 °C were selected. The results were compared with samples calcined at 120 and 200 °C and having the maximum moisture content.

Effect of the dehydration temperature of Al₂O₃ on its ability towards chlorination with carbon tetrachloride

The chlorination temperature of Al₂O₃ is an important parameter of synthesis of Cl-Al₂O₃ and should be selected in such a way during chlorination that a Cl-containing precursor interacts only with surface centres of Al₂O₃ and reactions with bulky groups in Al₂O₃ should be avoided. This is related to the fact that massive AlCl₃ species are sublimated to Al₂Cl₆ already at 180 °C [29] and evaporate from the γ -Al₂O₃ – CCl₄ reaction system as vapours [13, 29]. The intense generation of AlCl₃ and the removal of its vapours for systems based on γ -Al₂O₃ was noted at temperatures higher than 350 °C [13], and for those with χ -Al₂O₃ – above 450 °C [30]. Considering this fact, this paper carried out chlorination of Al₂O₃ samples with carbon tetrachloride at 350 °C. Table 2 gives chlorine content in samples and main textural and acid characteristics.

Data analysis of chlorine content in Cl-Al₂O₃ samples demonstrates that it does not linearly depend on the temperature of thermal treatment of gibbsite and correlates with changes of moisture content of samples in temperature regions of χ -Al₂O₃ existence. Thus, gibbsite samples with calcination temperatures of 120 and 200 °C and high moisture content (about 0.3 g H₂O/g Al₂O₃) sorb a large amount of chloride ions that varies within 4.7–4.9 mass %. It should be noted that chlorination of gibbsite samples is accompanied by the transformation of gibbsite to χ -Al₂O₃ caused by a higher temperature of chlorination (350 °C) compared to the temperature of their thermal treatment. The consequence of phase transformation of gibbsite to χ -Al₂O₃ is the observed dispersion of species and the development of the surface and volume of mesopores in 4.9Cl/ χ -Al₂O₃-200 sample (see Table 2).

A threefold decrease of moisture content in samples of gibbsite calcined at 300 and 400 °C causes a weak impact on the ability of χ -Al₂O₃ towards sorption of chloride ions. However, a decrease in moisture content of χ -Al₂O₃ in 10–15 times resulting from gibbsite calcination at 500 and 600 °C causes a decrease in its ability towards sorption of chloride ions from CCl₄ in 1.5–2 times. Chlorine content in 2.7Cl/ χ -Al₂O₃-500 sample is twice lower, in 4.4Cl/ χ -Al₂O₃-400 – comparable, in 5.2Cl/ χ -Al₂O₃-300 – some higher than in 4.9Cl/ χ -Al₂O₃-200 sample with a low temperature of thermal treatment of gibbsite. It should be noted that there is a trend to decreasing chlorine content within 300–500 °C temperature range, and on the contrary, to an increase in chlorine content in Cl/ χ -Al₂O₃-*T* in the 500–600 °C range with increasing the temperature of thermal treatment of gibbsite. Analysing the effect of moisture content in gibbsite and χ -Al₂O₃ samples on their ability towards sorption of chloride ions, a number of important conclusions can be made. Firstly, crystalline water in the composition of gibbsite (Al(OH)₃ · *n*H₂O) with calcination temperatures of 120 and 200 °C has a negative impact on the ability of gibbsite to sorb chloride ions upon the interaction with CCl₄ at 350 °C, though this effect is minor. Secondly, the generation of χ -Al₂O₃ from gibbsite at 300 °C has a positive effect on sorption capac-

ity for chloride ions. Thirdly, a decrease in the specific surface area of χ -Al₂O₃ resulting from increasing calcination temperature leads to a decrease in chlorine content and chloride ion density in Cl/ χ -Al₂O₃-*T* apparently because of a decrease in the concentration of functional groups in the χ -Al₂O₃ surface. The density of Cl ions in 5.2Cl/ χ -Al₂O₃-300, 4.4Cl/ χ -Al₂O₃-400 and 2.7Cl/ χ -Al₂O₃-500 samples was 3, 2.6 and 2 pcs/nm², respectively. This value is 1.5–2 times higher than the concentration of acid sites registered by the NH₃-TPD method in appropriate χ -Al₂O₃-*T* samples. Fourthly, the transformation of even a minor fraction of boehmite into γ -Al₂O₃ after calcination of gibbsite at 600 °C also favours sorption of chloride ions, which may also be related to a change in acid properties of the surface of alumina.

Effect of the moisture content of Al₂O₃ on textural characteristics of Cl/ χ -Al₂O₃

Textural characteristics of chlorinated χ -Al₂O₃ samples obtained from gibbsite with calcination temperatures in the 300–500 °C range vary relatively to non-chlorinated samples. A decrease in the specific surface area and the average mesopore size is a general trend (see Table 2). A reduction in the specific surface area for Cl/ χ -Al₂O₃-*T* samples compared to appropriate χ -Al₂O₃-*T* samples was about 20–30 % with decreasing the average pore size in 1.5–2 times and retaining mesopore volume. For 3.5Cl/ χ -Al₂O₃-600 sample, there was a trend towards an increase in mesopore volume from 0.26 to 0.3 cm³/g with retaining surface area and mesopore size.

Low-temperature nitrogen adsorption isotherms of chlorinated samples, examples of which are given in Fig. 5, *a* refer to the IV type but have several peculiarities compared to those for non-chlorinated χ -Al₂O₃ types. In particular, with the identical relative pressure of adsorbate, Cl/ χ -Al₂O₃-*T* samples absorb a lower volume of adsorbate than χ -Al₂O₃-*T* with the same calcination temperature. There is a weak trend towards a shift of the hysteresis loop in the direction of high pressures of adsorbate for chlorinated samples when comparing nitrogen adsorption isotherms in Cl/ χ -Al₂O₃-*T* and

χ -Al₂O₃-*T*. The hysteresis loop in Cl/ χ -Al₂O₃-*T* with a higher temperature of gibbsite calcination is shifted to the area of greater pressures, which points out at a change in the shape and pore size in samples. Pores with the sizes of 3–4 nm prevail in Cl/ χ -Al₂O₃-*T* samples (see Fig. 5, *b*); they account for a somewhat greater volume than in non-chlorinated χ -Al₂O₃-*T* types with the same calcination temperature (see Fig. 4, *b*). It should also be noted that the surface of pores with a size of 3.5–80 nm in Cl/ χ -Al₂O₃-*T* samples obtained from gibbsite with calcination temperature of 200–400 °C makes a minor contribution into the total specific surface area of samples. Their specific surface areas calculated according to BET and BJH methods are different by 70–80 %, from which it may be concluded that Cl/ χ -Al₂O₃-*T* samples are microporous. The difference in surface values according to BET and BJH for Cl/ χ -Al₂O₃-500 and Cl/ χ -Al₂O₃-600 samples is almost absent, therefore, the number of thin pores is minimum. Thus, a fraction of small mesopores with a size up to 3.5 nm increases during chlorination of χ -Al₂O₃-*T* with carbon tetrachloride apparently due to surface dissolution with the transformation of alumina to AlCl₃ and precipitation of the latter in the same or greater size mesopores.

Chlorination of χ -Al₂O₃ samples obtained by thermal treatment of gibbsite with carbon tetrachloride at 300–600 °C causes degradation of the near-surface layer of χ -Al₂O₃ species at 350 °C, though particle morphology in Cl/ χ -Al₂O₃ and χ -Al₂O₃ remains identical. For example, 3.5Cl/ χ -Al₂O₃-600 sample obtained from gibbsite with calcination temperature of 600 °C comprises χ -Al₂O₃ crystallites with implicitly distinct faceting along the main crystallographic directions (Fig. 6, *a*). Cavities, pores and facet structure of the species are clearly seen in images with a magnification of 250 000 (see Fig. 6, *b*). Pore size somewhat increases compared to the non-chlorinated sample being 2–5 nm. The near-surface layer with a thickness of not more than 5 nm has an amorphous structure.

Thus, the data of nitrogen low-temperature adsorption and TEM well agree among themselves attesting to the textural characteristics of Cl/ χ -Al₂O₃ samples and particle morphology versus gibbsite pre-treatment temperature and moisture content therein.

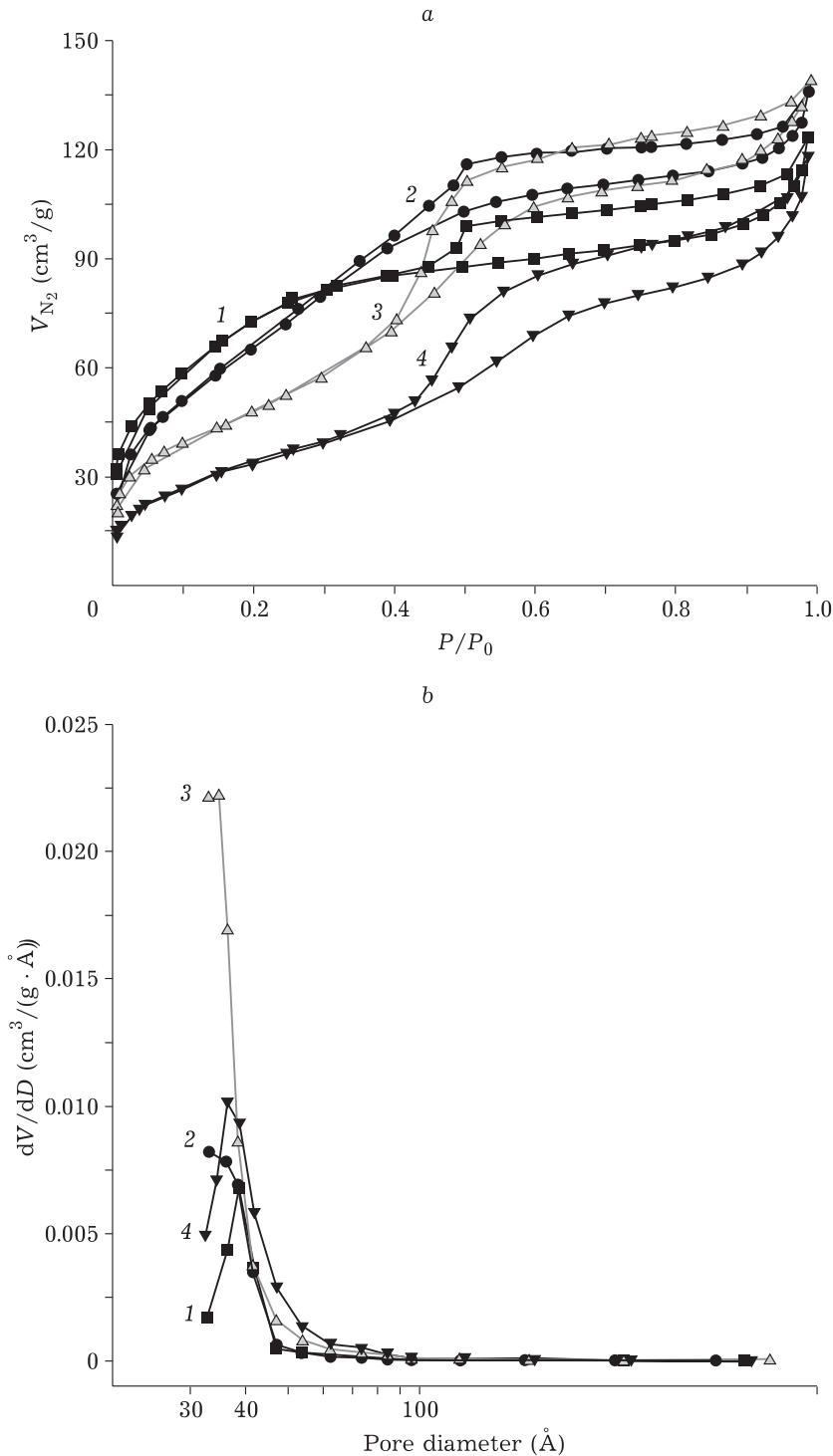


Fig. 5. Adsorption isotherms (a) and differential pore size distribution (b) of chlorinated samples of gibbsite exposed to preliminary calcination at temperatures of 200 (1), 300 (2), 500 (3), and 600 (4).

Thermal stability of $Cl-\chi-Al_2O_3$ samples

The thermal stability of $Cl/\chi-Al_2O_3-T$ samples in an oxygen-containing medium was studied *via* the TG-DTA method. Figure 7 demonstrates the results for four samples obtained

from gibbsite with pre-treatment temperatures of 200, 300, 500, and 600°C that are different in moisture content. The TG curves of samples with gibbsite calcination temperatures of 200 and 300°C have two mass loss stages with maxima at 90 and 520–525°C accompanied by

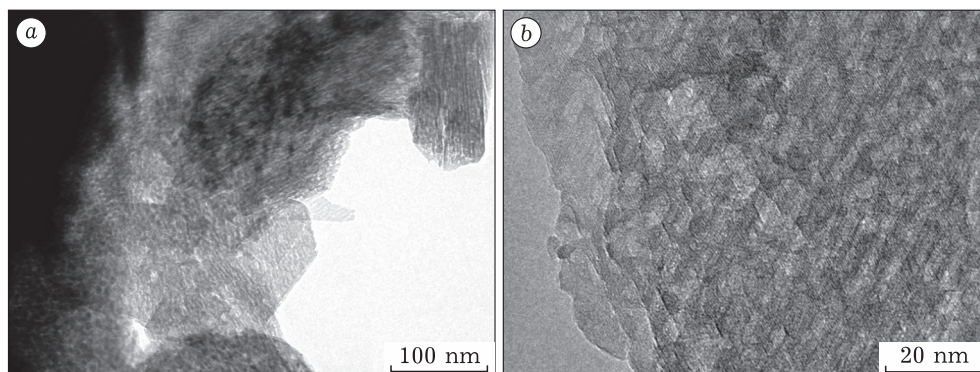


Fig. 6. TEM images of Cl/ χ -Al₂O₃-600 sample obtained by chlorination of gibbsite with carbon tetrachloride at preliminary heat-treatment temperature of 600 °C. An increase of 10k (a), 250k (b).

distinct endo-effects at 135 и 537–542 °C (see Fig. 7, a and b). It should be noted that mass loss in the area of 520–525 °C is approximately 2–3 higher than in the region of 90 °C for both samples. The first peak (90 °C) is associated with adsorbed water loss. The mass loss at 520–525 °C was also present in the TG curve of gibbsite but had twice lower values, whereas the peaks at 235 and 325 °C disappeared. Thus, during chlorination of gibbsite samples with calcination temperatures of 200 and 300 °C, the process of its dehydration (235 °C, see Fig. 2) and transformation to χ -Al₂O₃ (325 °C, see Fig. 2) has completely ended, which is driven by a higher temperature of its chlorination (350 °C). A peak in the area of 520–525 °C is apparently due to two processes, such as the removal of surface chloride ions and transformation of boehmite to γ -Al₂O₃.

The effects found during DTA analysis of Cl/ χ -Al₂O₃-500 and Cl/ χ -Al₂O₃-600 samples based on gibbsite with calcination temperatures of 500 and 600 °C are somewhat different from effects typical for chlorinated samples based on gibbsite subjected to treatment at 200 and 300 °C. They demonstrated by a shift of low-temperature mass loss from 90 to 110–120 °C, endo-effect temperature from 135 to 155 °C, and lower mass loss in the 300–600 °C temperature range than for Cl/ χ -Al₂O₃-300, 3.4–3.8 mass % instead of 8–9.2 mass % (see Fig 7, c and d).

Comparing the described peculiarities observed in DTA of gibbsite and chlorinated samples on its basis, the following conclusions can be made. A peak at temperatures near 90–120 °C in TG curves of Cl/ χ -Al₂O₃-T samples

is due to liberation of HCl and H₂O. Moreover, HCl release is caused by hydrolysis of surface >Al-Cl groups in adsorbed water vapours; it occurs at 90–200 °C. Simultaneously with HCl liberation, >Al-Cl groups turn into >Al-OH. The mass loss at a temperature above 300 °C, in this case, is associated with water removal resulting from condensation of appropriate groups in Al₂O₃. In addition, weak exo-effects at 283 and 440–490 °C that are apparently due to the removal of carbon accumulated in the surface of chlorinated samples during chlorination by carbon tetrachloride appear in DTA curves of Cl/ χ -Al₂O₃-T samples.

Surface acid properties of Cl-Al₂O₃ samples

The NH₃-TPD method is utilized to determine the total surface acidity of ceramic materials driven by proton-donor (Bronsted) and electron-acceptor (Lewis) surface sites [31]. It is believed that the number of sites that are able to chemisorb ammonia is comparable with the total concentration of Bronsted sites with a vibration frequency of OH groups near 3688 cm⁻¹ and medium strength Lewis sites with a vibration frequency of CO near 2200–2210 cm⁻¹ and the heat of adsorption of CO near 35–38 kJ/mol [31]. Weak Lewis sites with the frequency of $\nu(\text{CO}) = 2180\text{--}2195\text{ cm}^{-1}$ and proton groups with low acidity ($\nu(\text{OH}) = 3750\text{--}3780\text{ cm}^{-1}$) form weak physical bonds with the ammonia molecule under NH₃-TPD conditions. This results in its removal at the sample purge stage at 100 °C [31].

Figure 8 illustrates the NH₃-TPD profile of

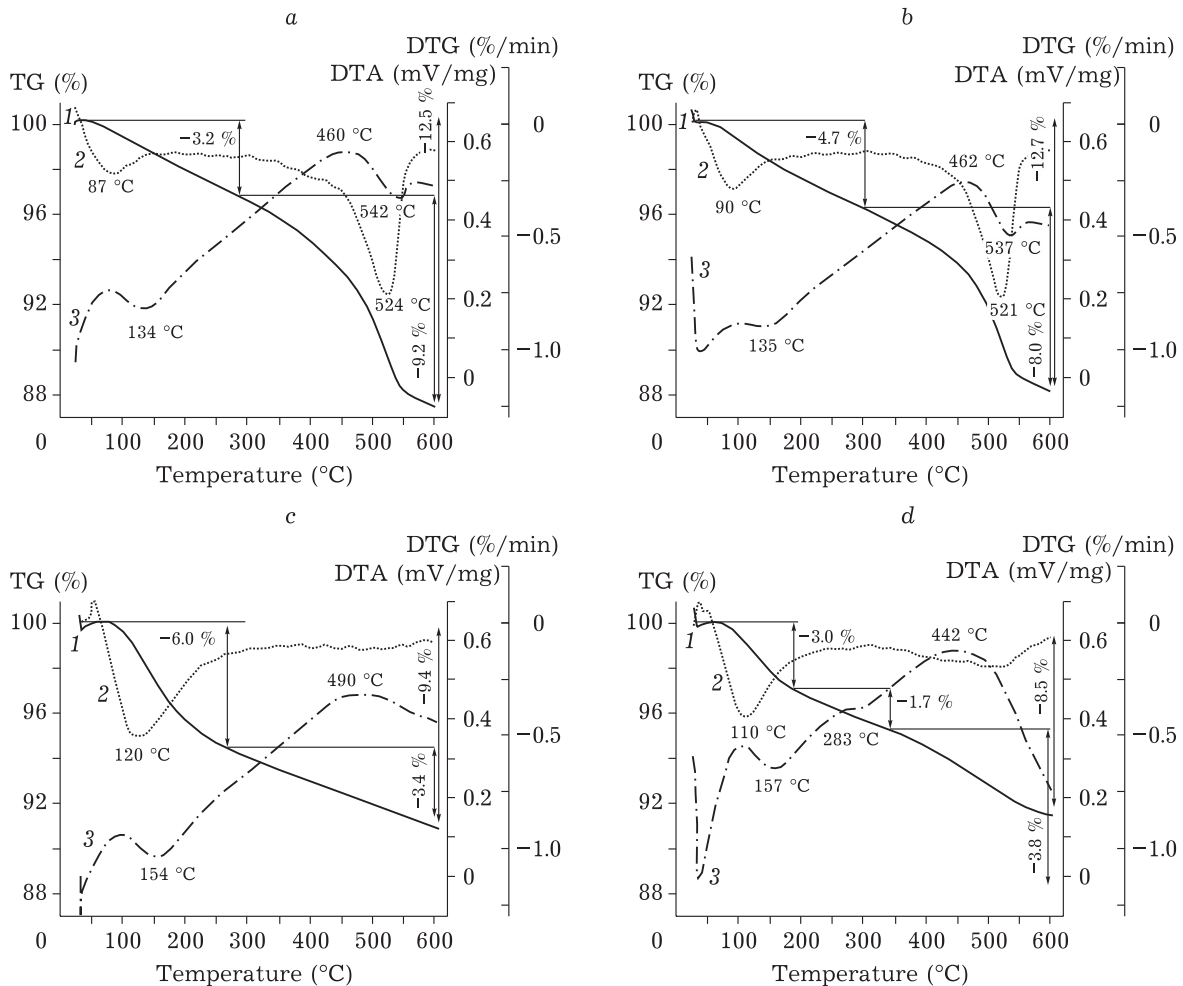


Fig. 7. TG (1), DTG (2) and DTA (3) curves for chlorinated samples of $\text{Cl}/\chi\text{-Al}_2\text{O}_3\text{-T}$ produced from gibbsite with pre-heat treatment temperature of 200 (a), 300 (b), 500 (c), and 600 °C (d).

non-modified $\chi\text{-Al}_2\text{O}_3$ and chlorinated $\text{Cl}/\chi\text{-Al}_2\text{O}_3\text{-T}$ samples obtained from gibbsite with different thermal treatment temperatures. Tables 1 and 2 give the total content of acid sites according to the $\text{NH}_3\text{-TPD}$ data.

A broad asymmetric peak of ammonia desorption with a distinct maximum in the region of 390 °C and a shoulder at 520 °C characterize $\chi\text{-Al}_2\text{O}_3$ sample in $\text{NH}_3\text{-TPD}$ experiments. The observed maxima correspond to ammonia desorption from acid sites with different strengths. According to ammonia chemisorption energy, the sites can be conventionally divided into Lewis acid sites (LAS, aprotic sites) and Bronsted acid sites (BAS, proton-donor sites), respectively. Lewis acid sites of average strength with ammonia desorption energy of 110–150 kJ/mol make a greater contribution into sample total

acidity. Their fraction accounts for about 70 % of the number of acid sites observed according to $\text{NH}_3\text{-TPD}$. Ammonia desorption energy of over 150 kJ/mol characterizes proton sites, while their structure corresponds to bridged hydroxyl groups with the maximum acidity, according to the data of [31].

Results of the $\text{NH}_3\text{-TPD}$ experiments of $\text{Cl}/\chi\text{-Al}_2\text{O}_3\text{-T}$ samples obtained for gibbsite with calcination temperatures of 200, 300 and 500, 600 °C are substantially different. Firstly, ammonia absorption is almost absent in the 300–550 °C range during $\text{NH}_3\text{-TPD}$ experiments of $\text{Cl}/\chi\text{-Al}_2\text{O}_3\text{-200}$ and $\text{Cl}/\chi\text{-Al}_2\text{O}_3\text{-300}$ samples. The amount of ammonia absorbed in this region is not more than 30 $\mu\text{mol/g}$ indicating the minor amount of LAS of average strength and strong BAS in $\text{Cl}/\chi\text{-Al}_2\text{O}_3\text{-200}$ and $\text{Cl}/\chi\text{-Al}_2\text{O}_3\text{-300}$.

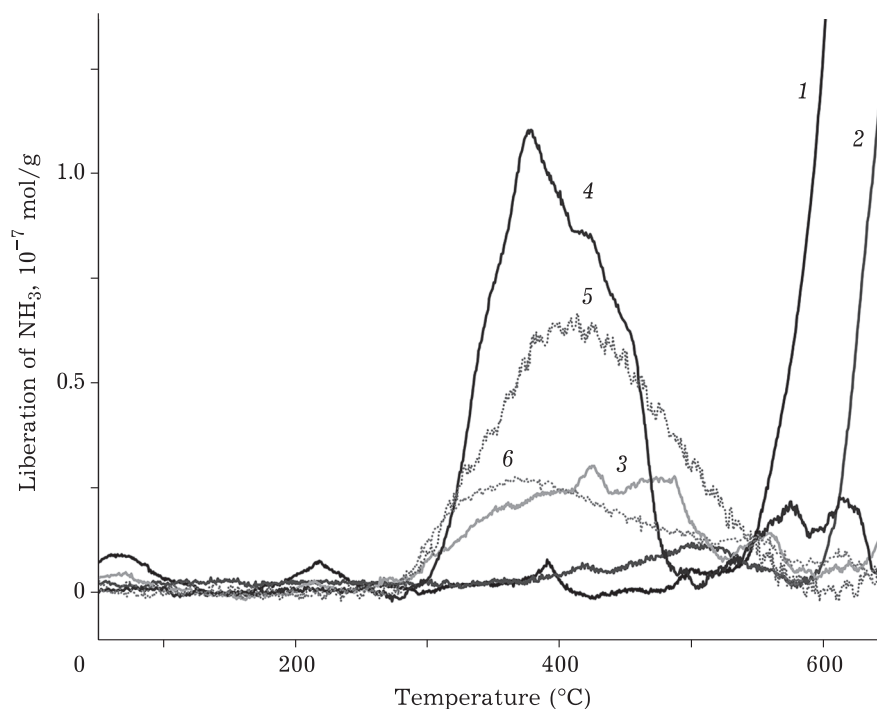


Fig. 8. NH_3 -TPD spectra for $\text{Cl}/\chi\text{-Al}_2\text{O}_3\text{-}T$ samples chlorinated in a flow of CCl_4 and derived from gibbsite previously calcined at 200 (1), 300 (2), 500 (3), and 600°C (4). For comparison, spectra of $\chi\text{-Al}_2\text{O}_3\text{-}600$ (5) and $0.2\text{Cl}/\chi\text{-Al}_2\text{O}_3\text{-}500$ (6) obtained by impregnation in CCl_4 followed by calcination at 500°C are presented

The $\text{Cl}/\chi\text{-Al}_2\text{O}_3\text{-}500$ sample desorbs ammonia in the same temperature region (300–600°C), as the non-chlorinated sample, but its amount is almost twice lower than for a non-chlorinated sample. In addition, BAS concentrations in chlorinated and non-chlorinated $\chi\text{-Al}_2\text{O}_3\text{-}500$ samples are different in 5 times accounting for about 37 and 200 $\mu\text{mol/g}$, respectively.

The total concentration of acid sites increases in $\text{Cl}/\chi\text{-Al}_2\text{O}_3\text{-}600$ sample compared to a non-chlorinated sample (from 660 to 820 $\mu\text{mol/g}$) mainly due to increasing the number of LAS amount, while there is no BAS with ammonia desorption temperature of 480–550°C in its spectrum, however, new BAS with ammonia desorption temperature of 550–600°C and heat of desorption above 180 kJ/mol appear. It should be noted that when $\chi\text{-Al}_2\text{O}_3\text{-}500$ sample impregnated with carbon tetrachloride was calcined under static conditions at 350°C, almost in 13 times lower chlorine than in $2.7\text{Cl}/\chi\text{-Al}_2\text{O}_3\text{-}500$ sample obtained at the same chlorination temperature but under flow conditions was stabilized in its surface. However, $2.7\text{Cl}/\chi\text{-Al}_2\text{O}_3\text{-}500$ and $0.2\text{Cl}/\chi\text{-Al}_2\text{O}_3\text{-}500$ (stat)

samples are characterized by close spectra of ammonia desorption; the total content of the observed sites is comparable (about 350 $\mu\text{mol/g}$). The only difference is a mild trend towards a greater concentration of weak LAS in $0.2\text{Cl}/\chi\text{-Al}_2\text{O}_3\text{-}500$ (stat) and BAS with heat for the ammonia desorption of 150 kJ/mol.

Secondly, in spectra of $\text{Cl}/\chi\text{-Al}_2\text{O}_3\text{-}200$ and $\text{Cl}/\chi\text{-Al}_2\text{O}_3\text{-}300$ samples, low-temperature peaks corresponding to weak sites with low heat for the desorption of ammonia (less than 80 kJ/mol) appear in NH_3 -TPD curves at 80 and 220°C.

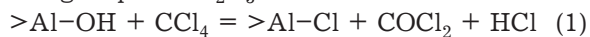
Thirdly, the main peculiarity of NH_3 -TPD spectra for $\text{Cl}/\chi\text{-Al}_2\text{O}_3\text{-}200$ and $\text{Cl}/\chi\text{-Al}_2\text{O}_3\text{-}300$ samples is intense peaks with maxima near 680–700°C. As a rule, peaks in the specified temperature region of NH_3 -TPD are not considered in the literature, as they may be related to both phase transitions of Al_2O_3 and the formation of AlN [32, 33]. The transformation of Al_2O_3 and AlCl_3 to AlN requires temperatures above 600°C [32, 33] and reducing media in case of Al_2O_3 [33]. A high-temperature peak for non-chlorinated and chlorinated $\chi\text{-Al}_2\text{O}_3\text{-}T$ samples with temperatures of pre-calcination of gibbsite

of 500°C and higher was also observed, but its intensity was very low.

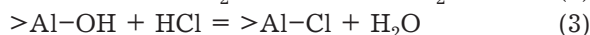
Thus, the NH₃-TPD data attests to the dependence of acid characteristics of Cl/ χ -Al₂O₃ samples on gibbsite pre-treatment temperature and moisture content therein. Weak LAS with a heat of desorption lower than 80 kJ/mol are generated resulting from a high moisture content in gibbsite samples. According to the data of [31], it is impossible to observe weak LAS ($\nu(\text{CO}) = 2180\text{--}2195\text{ cm}^{-1}$) and proton groups with mild acidity ($\nu(\text{OH}) = 3750\text{--}3780\text{ cm}^{-1}$) using NH₃-TPD. Therefore, their generation in samples with low gibbsite calcination temperature is not eliminated by us. There is a trend towards increasing a fraction of LAS of average strength and decreasing the concentration of BAS with heat for the ammonia desorption of about 150 kJ/mol as the moisture content decreases in a non-chlorinated sample. The content of strong BAS did not depend on the residual moisture in the case of non-chlorinated gibbsite samples with calcination temperature of 500°C and higher.

Chemism of surface chlorination of Cl-Al₂O₃ samples

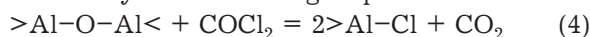
The interaction of gaseous CCl₄ with surface >Al-OH groups of χ -Al₂O₃ proceeds at chlorination temperatures up to 300–350°C inclusive, as demonstrated earlier [30]. A change in acid properties of the surface is mainly caused by the formation of LAS, such as >Al-Cl. Carbon tetrachloride decomposes to COCl₂ and HCl at temperatures of 400°C and above due to acid OH groups of Al₂O₃



and to Cl₂ and carbon resulting from thermal hydrolysis (CCl₄ = Cl₂ + C). Thus, COCl₂, HCl, and Cl₂ are essentially chlorinating reagents in the 400–500°C temperature range that are more reactive and interact both with terminal >Al-OH groups:



and bulky >Al-O-Al< groups of alumina:



to form surface >Al-Cl groups, new proton >Al-OH sites, and AlCl₃ nanoparticles. The modification

of χ -Al₂O₃ surface by chloride ions in the 300–400°C range proceeds *via* a mixed mechanism.

Paper [34] found that HCl, COCl₂, CO₂, and H₂O are generated during chlorination of χ -Al₂O₃ with carbon tetrachloride even at a temperature of 200°C. Since COCl₂ may hydrolyze to form an additional amount of HCl (COCl₂ + H₂O = CO₂ + 2HCl [35]), it remained unclear, whether water vapours affected the content of chlorine introduced by chlorination of functional groups of χ -Al₂O₃ with carbon tetrachloride and acid properties of Cl/ χ -Al₂O₃. For this purpose, the effect of moisture content of gibbsite and χ -Al₂O₃ obtained on its basis on chlorine content and the regularity of generating acid properties of the surface was explored.

As discussed above, moisture content has a non-linear effect on the amount of adsorbed chlorine. In particular, χ -Al₂O₃ samples from gibbsite with calcination temperature of 300°C can sorb chloride ions best of all. Both decreasing gibbsite calcination temperature to 200°C and its increasing to 400–600°C lead to a reduction of chlorine content in Cl/ χ -Al₂O₃ -*T* samples. In addition, there is a trend towards a decrease in chlorine content with an increase in gibbsite calcination temperature from 300 to 500°C. Meanwhile, however, the density of acid sites observed in NH₃-TPD decreases. The specified trends may be changed by two methods. Firstly, this can be done through the participation in χ -Al₂O₃ chlorination of vapours of gaseous HCl generated resulting from COCl₂ hydrolysis with water vapours, therefore, chlorine content in samples should be proportional to χ -Al₂O₃ moisture content. Secondly, this can be achieved through the difference in the concentration of functional >Al-OH groups on the χ -Al₂O₃ surface, herewith, the density of the specified groups should be higher in samples with lower dehydration temperatures and higher specific surface areas. The generated >Al-Cl sites are apparently weak LAS. The role of medium and strong acid sites in chlorination is enhanced with increasing calcination temperature. Thus, the observed regularities of a change in acid properties of chlorinated alumina are explained by both chemism of reactions proceeding during the interaction of CCl₄ and HCl with surface terminal

>Al-OH and the density of >Al-OH functional groups.

CONCLUSION

A comparative study of the chemical composition of chlorinated alumina obtained by chlorination of χ -alumina with carbon tetrachloride and its morphological, textural, structural, and acid properties allows making a conclusion that residual moisture has a substantial effect on listed properties of chlorinated alumina.

Chlorination of χ -Al₂O₃ samples produced by gibbsite thermal treatment (at 300–600 °C), carbon tetrachloride at 350 °C causes destruction of the near-surface layer with a thickness of not more than 5 nm in χ -Al₂O₃ species; their size and shape do not vary, and new ones with a size of 2–5 nm appear.

The NH₃-TPD data indicate that weak Lewis acid sites (LAS) with heat of desorption lower than 80 kJ/mol are formed in chlorinated samples obtained on the basis of gibbsite with calcination temperature of 200–300 °C and high residual moisture contents. There is a trend towards to increasing a fraction of LAS of an average strength and decreasing the concentration of BAS with heat for the desorption of ammonia of 150 kJ/mol when reducing moisture content of non-chlorinated samples. The content of BAS with heat for the desorption of ammonia of over 180 kJ/mol almost did not depend on moisture content of non-chlorinated samples with gibbsite calcination temperatures of 500 °C and above.

Gibbsite calcination temperature, variation of which adjusted moisture contents in gibbsite and χ -Al₂O₃ determined the peculiarities of acid properties of χ -Al₂O₃, in particular, the density of OH groups, and chlorinated samples on its basic. Chemism of the reaction between carbon tetrachloride and acid sites in alumina was also different, since CCl₄ and HCl (COCl₂ hydrolysis product) took part in chlorination of samples with a high moisture content, and with low one – only CCl₄.

Acknowledgements

The work was carried out with the financial support of SB RAS and FANO of Russia (the

program II.2P/V.45-12, project 0303-2015-0006).

The authors are grateful to T. Ya. Efimenko for help in determining adsorption characteristics and to G. S. Litvak for carrying out the DTA.

REFERENCES

- 1 US Pat. No. 3047514, 1962.
- 2 Basset J., Figueras F., Mathieu M. V., Prettre M., *J. Catal.* 1970. Vol. 16. P. 53–61.
- 3 US Pat. No. 3892683, 1975.
- 4 Comet D., Goupil J.-M., Szabo G., Poirier J.-L., Clet G., *Appl. Catal. A* 1996. Vol. 141. P. 193–205.
- 5 Arena F., Frusteri F., Mondello N., Giordano N., *J. Chem. Soc., Faraday Trans.* 1992. Vol. 88. P. 3353–3356.
- 6 Goble A. G., Lawrance P. A., Proceedings of the 3rd International Congress on Catalysis. North-Holland, Amsterdam, 1964. P. 320.
- 7 Clet G., Goupil J. M., Szabo G., Cornet D., *Mol. Catal. A: Chem.* 1999. Vol. 148. P. 253–264.
- 8 Melchor A., Garbowski E., Mathieu M.-V., Primet M., *J. Chem. Soc., Faraday Trans.* 1. 1986. Vol. 82. P. 1893–1901.
- 9 Kytokivi A., Lindblad M., Root A., *J. Chem. Soc., Faraday Trans.* 1995. Vol. 91. P. 941–948.
- 10 Tanaka M., Ogasawara S., *J. Catal.* 1970. Vol. 16. P. 157–163.
- 11 Bailey R. R., Wightman J. P., *J. Colloid Int. Sci.* 1979. Vol. 70. P. 112–122.
- 12 Tanaka M., Ogasawara S., *J. Catal.* 1970. Vol. 16. P. 164–172.
- 13 Cai T., Liu S., Qu J., Wong S., Song Z., He M., *Appl. Catal. A: Gen.* 1993. Vol. 97. P. 113–122.
- 14 Garbowski E., Primet M., *J. Chem. Soc., Faraday Trans.* 1. 1987. Vol. 83. P. 1469–1476.
- 15 Marczewski M., Derewinski M., Malinowski S., *Can. J. Chem. Eng.* 1983. Vol. 61. P. 93–97.
- 16 Ayame A., Sawada G., Sato H., Zhang G., Ohta T., Izumizawa T., *Appl. Catal.* 1989. Vol. 48. P. 25–35.
- 17 Ayame A., Sawada G., *Bull. Chem. Soc. Jpn.* 1989. Vol. 62. P. 3055–3060.
- 18 Busca G., *Adv. Catal.* 2014. Vol. 57. P. 320–402.
- 19 Kul'ko E. V., Ivanova A. S., Budneva A. A., Paukshtis E. A., *Kinetika i Kataliz.* 2005. Vol. 46(1). P. 141–146.
- 20 Tsuchida T., Ishii T., Furuichi R., Haga H., *Thermochimica Acta.* 1979. Vol. 34 (1). P. 19–28
- 21 Bursian N. R. *Tekhnologiya Izomerizatsii Parafinovykh Uglevodorodov*, M.: Khimiya, 1985. P. 66–74.
- 22 McInroy A. R., Lundie D. T., Winfield J. M., Dudman C. C., Jones P., Parker S.F., Lennon D., *Catal.Today.* 2006. Vol. 114. P. 403–411.
- 23 Wells A. *Strukturnaya Neorganicheskaya Khimiya*, Vol. 2, Per. s angl., M.: Mir, 1987. 696 p.
- 24 Linsen B. G. *Stroenie i Svoistva Adsorbentov i Katalizatorov*, M.: Mir, 1973. 653 p.
- 25 Geits B., Ketsir Dzh., Shuit D., *Khimiya Kataliticheskikh Protessov*, M.: Mir, 1981. 342 p.
- 26 Chukin G. D., *Stroenie Oksida Alyuminiya i Katalizatorov Gidrobesserivaniya. Mekhanizmy Reaktsii*, M.: Paladin, 2010. 288 p.
- 27 Shkrabina R. A., Moroz E. M., Levitskii E. A., *Kinetika i Kataliz.* 1981. Vol. 22, No. 5. P. 293–1299.
- 28 Tsybulya S. V., Kryukova G. N., *Phys. Rew. B.* 2008. Vol. 7, No. 024112. P. 1–13
- 29 Perry's Chemical Engineering Handbook, 7th Ed., R. H.

- Perry, D. W. Green, J. O. Maloney (Eds.). McGraw-Hill, New York, 1984, Table 2–7.
- 30 Yashnik S. A., Shikina N. V., Salnikov A. V., Ishchenko A. V., Prosvirin I. P., Litvak G. S., Noskov A. S., *Catalysis for Sustainable Energy*. 2017. Vol. 4, No. 1. P. 36–51.
- 31 Yushchenko V. V., *Zhurnal Fizicheskoi Khimii*, 1997. Vol. 71, No. 4. P. 628–632.
- 32 Wang M.-Ch., Wu N.-Ch., Tasi M.-S., Liu. H.-Sh., *J. Crystal Growth*. 2000. Vol. 216 (1). P. 69–79.
- 33 You Y., Ito A., Tu R., Goto T., *Key Engineering Materials*. 2011. Vol. 484. P. 172–176.
- 34 Thomson J., Webb G., Witfield J. M., *J. Mol. Catal.* 1991. Vol. 67. P. 117–126.
- 35 Remi G., *Kurs Neorganicheskoi Khimii*, Vol. 1, V. V. Novoselova (Ed.), M.: Izd-vo inostr. lit., 1963. P. 920.